A Combined Spectrum Sensing and OFDM Demodulation Scheme

M. Heskamp, C. H. Slump
University of Twente, Faculty of EEMCS,
Signals and Systems Group (SaS),
P.O. box 217 - 7500 AE Enschede - The Netherlands
Phone: +31 53 489 2673 Fax: +31 53 489 1060
E-mail: m.heskamp@ewi.utwente.nl

***Abstract*—In this paper we propose a combined signaling and spectrum sensing scheme for cognitive radio that can detect in-band primary users while the networks own signal is active. The signaling scheme uses OFDM with phase shift keying modulated sub-carriers, and the detection scheme measures the deviation of each sub-carrier from a circular shape.**

I. Introduction

Cognitive radio is a promising new paradigm of radio spectrum access, in which unlicensed secondary users are allowed to transmit in licensed bands when the primary user is not using its spectrum. [1]. In order to gain acceptance by primary users a cognitive radio has to guarantee very low levels of interference to them. On the other hand, the cognitive radio network has to maintain a reasonable quality of service, in order to justify the increased hardware costs.

Because of the fairly weak isolation between the transmitter and receiver circuits in a mobile device, it is infeasible to perform sensitive spectrum sensing during the time that the transmitter of the device is active. This means that during the time that the cognitive radio network is using the spectrum primary users can not be detected by the transmitting device. Other nodes of the cognitive radio network can still perform sensing, but weak in-band primary user signals remain obscured by the networks own signal.

In [2] the concept of self-signal suppression for cognitive radio is introduced. In this work, it is proposes to reconstruct the transmitted signal from the received bits and an estimated channel response. The difference between this reconstructed signal and the actually received signal is an estimation of the primary user signal. In [3] a self-signal suppression method is described that uses complementary OFDM symbol couples or sensing pilot carriers.

In this paper we propose to use OFDM with differential phase shift keying (DPSK) on each sub-carrier for the cognitive radio physical layer signaling. This has two advantages. First, DPSK does not need channel equalization, so no training symbols and pilot sub-carriers are required. This makes it simpler to make a notch in the transmit spectrum on occupied frequencies. Secondly, the PSK modulation gives a typical circular constellation diagram, which is maintained during frequency selective fading and additive channel noise. However, the circular shape is disturbed if another signal is added. So by looking at the constellation diagram of the sub-carriers, the cognitive radio receiver can detect interference.

[1]This work is supported by the Dutch Ministry of Economic affairs BSIK funding project and is part of the FreeBand program.

II. Review of $\pi/4$-QPSK -OFDM signaling

Fig. 1 shows a block scheme of a $\pi/4$-QPSK OFDM demodulator. The complex baseband samples from the AD converters first go through the frame detector, which recognizes the start of a frame and performs coarse timing synchronization. This timing correction does not need to be accurate because the cyclic prefix provides some margin for error. Next the frequency offset is estimated and corrected. Also the frequency offset estimation has a margin for error, because the differential phase shift keying can correct a phase rotation up to $\pi/4$ radians.

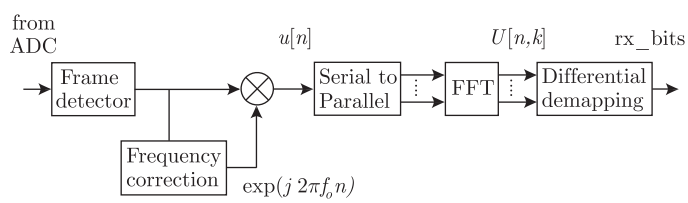

Fig. 1. OFDM receiver

Next, the stream of samples $u[n]$ is converted into blocks of FFT-size L samples, and the cyclic prefix is skipped. Next the L points FFT is performed, which gives the amplitude spectrum $U[n,k]$ in which k is the frequency bin number. Finally the sub-carriers are fed to the $\pi/4$-QPSK de-mapper, which converts the differential phase shift keying symbols back to bits.

Fig. 2a illustrates the phase transitions of the $\pi/4$-QPSK constellation if the previous symbol had a phase of zero. If the previous symbol was one of the other seven points, the phase transitions are similar. At the transmitter the complex symbols are formed according to

978-1-4244-4148-8/09/$25.00 ©2009
This full text paper was peer reviewed at the direction of IEEE Communications Society subject matter experts for publication in the IEEE "GLOBECOM" 2009 proceedings.

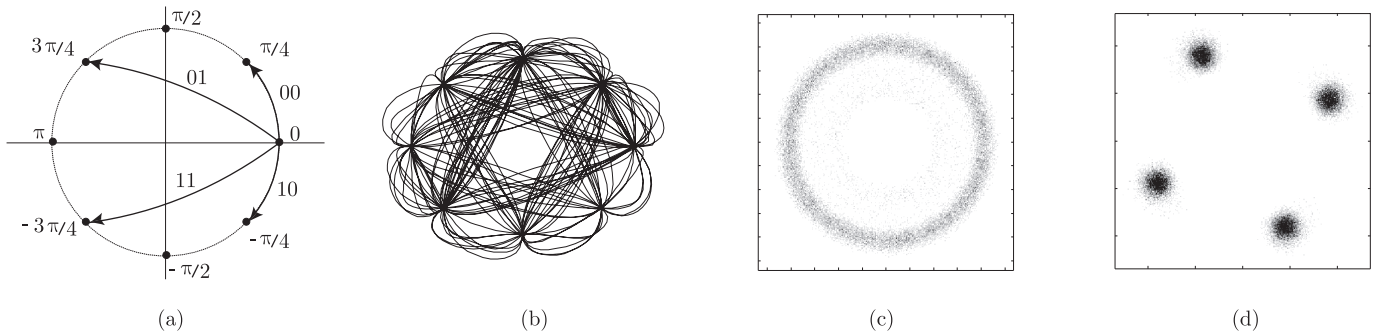

Fig. 2. $\pi/4$-QPSK constellation. (a) allowed phase transitions, (b) quadrature plot of continuous (interpolated) baseband signal, (c) received constellation diagram on one sub-carrier with some frequency and timing offset, (d) idem, after differential decoding.

$$
\begin{aligned}
c[0] &= \text{arbitray start symbol,} \\
c[n] &= c[n-1] \cdot \exp(j\Delta\varphi) \quad \text{for } n > 0, \\
\Delta\varphi &= \begin{cases} \pi/4 & \text{for} \quad b = 00 \\ 3\pi/4 & \text{for} \quad b = 01 \\ -\pi/4 & \text{for} \quad b = 10 \\ -3\pi/4 & \text{for} \quad b = 11 \end{cases}
\end{aligned} \tag{1}
$$

Because of the differential encoding, the first OFDM symbol in the frame can not contain information. This symbol is called the phase reference symbol, and can be chosen randomly.

The de-mapper in the receiver performs the inverse operation, according to

$$
\begin{aligned}
&\Delta\varphi = \arg(c[n] \cdot c[n-1]^{-1}) \quad \text{for } n > 0, \\
&\begin{aligned}
0 < \Delta\varphi < \pi/2 \quad &\Rightarrow \quad b = 00 \\
\pi/2 < \Delta\varphi < \pi \quad &\Rightarrow \quad b = 01 \\
-\pi/2 < \Delta\varphi < 0 \quad &\Rightarrow \quad b = 10 \\
-\pi < \Delta\varphi < -\pi/2 \quad &\Rightarrow \quad b = 11
\end{aligned}
\end{aligned} \tag{2}
$$

Now the interesting thing about this mapping scheme is that none of the phase transitions gives a path that goes right through zero, as can be seen in Fig. 2b. This results in a circular shaped constellation diagram at the receiver on each sub-carrier, as is shown in Fig. 2c. Because of some timing offset the shown constellation is rotating, so that the individual constellation points are not visible. After the differential decoding, the four constellation points become visible, as can be seen in Fig. 2d. Because of a small amount of frequency offset, the constellation is slightly rotated.

III. Detection scheme

Because of the typical circular shape of the constellation, we can easily detect interference by measuring the deviation from this shape. An efficient way to do this is by measuring the first and second order moments of the distribution, as shown in Fig. 3.

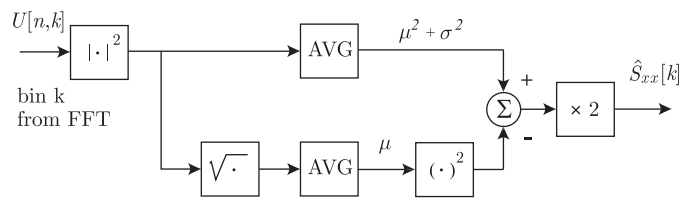

Fig. 3. Proposed detection scheme. The upper branch measures the spectrum, the lower branch cancels the self-signal.

The sub-carrier k can be written as

$$
U[n,k] \quad = \quad U_{\text{OFDM}}[n,k] \quad + \quad U_x[n,k], \tag{3}
$$

in which U_{OFDM} is the value of our own signal and U_x the contribution of possible primary user signals, noise and other interference. Noise can safely be assumed Gaussian, and because we are not synchronized with the primary user signal, we also assume it Gaussian, although the actual distribution is not important for our method. The probability distribution of $U[n,k]$ is the convolution of the distribution of U_{OFDM}, which is a circular line mass with radius μ, and the distribution of U_x, which is a two dimensional (quadrature) zero-mean Gaussian with variance $\sigma_{re}^2 + \sigma_{im}^2 = 2\sigma^2$. The resulting distribution has the shape of a ring, similar as shown in Fig. 2c. If we take the absolute value of $U[n,k]$ we get a Ricean distribution [4], which can be approximated by a Normal distribution

$$
|U[n,k]| \quad \sim \quad \mathcal{R}\text{ice}(\sigma,\mu) \quad \approx \quad \mathcal{N}(\mu,\sigma^2). \tag{4}
$$

If we assume the transmitted PSK modulated sub-carriers to have a magnitude of one we have

$$
\mu \quad = \quad |H[k]|, \tag{5}
$$

in which $|H[k]|$ is the attenuation caused by pathloss and fading. For the variance we have

978-1-4244-4148-8/09/$25.00 ©2009
This full text paper was peer reviewed at the direction of IEEE Communications Society subject matter experts for publication in the IEEE "GLOBECOM" 2009 proceedings.

$$\sigma^2 \;=\; \hat{S}_{xx}[k]/2, \tag{6}$$

in which $\hat{S}_{xx}[k]$ is our desired spectrum estimation. The factor half can be intuitively explained by the fact that by taking the absolute value, we effectively discarded the power of one of the two quadrature channels. If we average $|U[k]|$ over time we get

$$\begin{aligned} \langle\ |U[n,k]|\ \rangle \;&=\; \mu \quad \text{and} \\ \langle\ |U[n,k]|^2\ \rangle \;&=\; \mu^2+\sigma^2, \end{aligned} \tag{7}$$

so we have

$$\hat{S}_{xx}[k] \;=\; 2\left(\langle\ |U[k]|^2\ \rangle \;-\; \langle\ |U[k]|\ \rangle^2\right). \tag{8}$$

IV. Simulation Results

In Fig. 4 we compare our method with the Welch spectrum estimation. Fig. 4a shows the spectrum of four primary user signals, generated by simulation. From left to right in Fig. 4a, we first have a wide-band single-carrier $\pi/4$-QPSK signal with a relative bandwidth of 1/16, and a root raised cosine roll-off of 0.35. Next we have a non modulated carrier wave, a narrow-band QAM16 signal and an analog FM signal. The $\pi/4$-QPSK and QAM16 signal are modulated with pseudo random bits and the FM signal with a real audio fragment containing some music.

Fig. 4b shows the same spectrum, but now the cognitive radio signal is active. The four primary users signals are also present, but they are obscured by the cognitive radio signal.

In this simulation. the bandwidth of the cognitive radio's OFDM signal is 1/4 of the digital IF bandwidth, so that we have some freedom for frequency shifting and digital filtering. The OFDM signal uses 256 sub-carriers, loaded with differential $\pi/4$-QPSK symbols, a cyclic prefix of 64 points, and no pilot carriers. Coarse timing and frequency correction was done with four training symbols at the start of each frame. After the training symbols, each frame contained 100 data OFDM symbols with pseudo random data. As becomes clear from the figure, the OFDM signal largely overshadows the primary user signals. Only the empty carrier and the FM signal are still visible.

For Fig. 4a and b we used a Welch power spectral density estimator with an FFT size of 4096 points, a Gaussian window with $\alpha = 4$ and an autoregressive averager with $N = 100$.

Before the OFDM demodulator and spectrum sensing algorithm, we down-sample the signal with a factor four, which gives the spectra shown in Fig. 4c and d, which are also made with an FFT size of 4096 points. Fig. 4c shows just the four primary user signals, and Fig. 4d the primary user signals and the cognitive radio signal.

Fig. 4f is equivalent to Fig. 4d, but here the Welch estimator is replaced by the proposed method. As can be seen from this result, the self-signal is completely canceled, and the four primary user signals are clearly visible.

Fig. 4e is added for comparison. This sub-figure is equivalent to Fig. 4c, i.e. only primary user signals. To make the comparison fair, Fig. 4e uses the Welch method with an FFT size of 256 and no tapering window. As becomes clear from these results, a disadvantage of our method is the absence of a tapering window, which results in some leakage. However, for detection of primary user signals this leakage may not be a large problem.

V. Effect of residual frequency offset

In practice, the frequency synchronization between the transmitter and receiver is never perfect, which will result in a frequency offset. In most practical systems, this frequency offset is estimated with training symbols and then compensated by a frequency shift. If the residual offset f_o is much smaller than the sub-carrier spacing Δf it will no longer influence performance.

The spectrum sensing system described in this paper is also sensitive for frequency offset, because it will give an extra noise term. We can write the OFDM signal in the frequency domain as

$$U[k] \;=\; \sum_{i=0}^{L-1} c[i]\ \mathrm{sinc}(i-k-\frac{f_o}{\Delta f}). \tag{9}$$

If the frequency offset is zero, $U[k]$ only depends on symbol $c[k]$, but if there is frequency offset, it will depend on a weighted sum of all sub-carriers. This will result in a self-noise component.

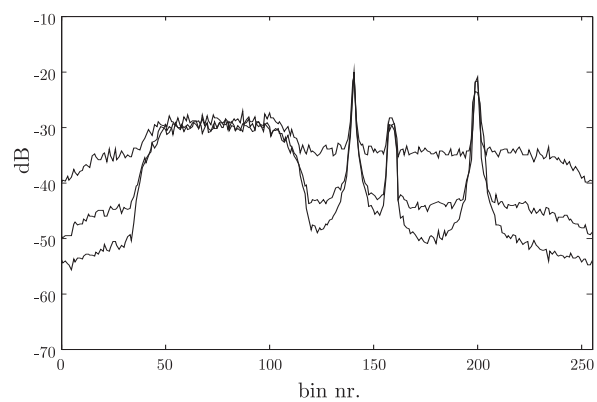

Fig. 5. Results with a frequency offset of $f_o/\Delta f$ = 0.1, 0.03 and 0.01 respectively from top to bottom.

Fig. 5 shows how the noise floor increases if a frequency offset is applied. We can find a theoretical value for the self-noise caused by frequency offset if we replace the time averaging operator in (8) by the mathematical expectation operator

$$\hat{S}[k] \;=\; 2\left(\mathrm{E}\left\{|U[k]|^2\right\} \;-\; \mathrm{E}\left\{|U[k]|\right\}^2\right). \tag{10}$$

The first term in (10) can be found by inserting (9)

978-1-4244-4148-8/09/$25.00 ©2009
This full text paper was peer reviewed at the direction of IEEE Communications Society subject matter experts for publication in the IEEE "GLOBECOM" 2009 proceedings.

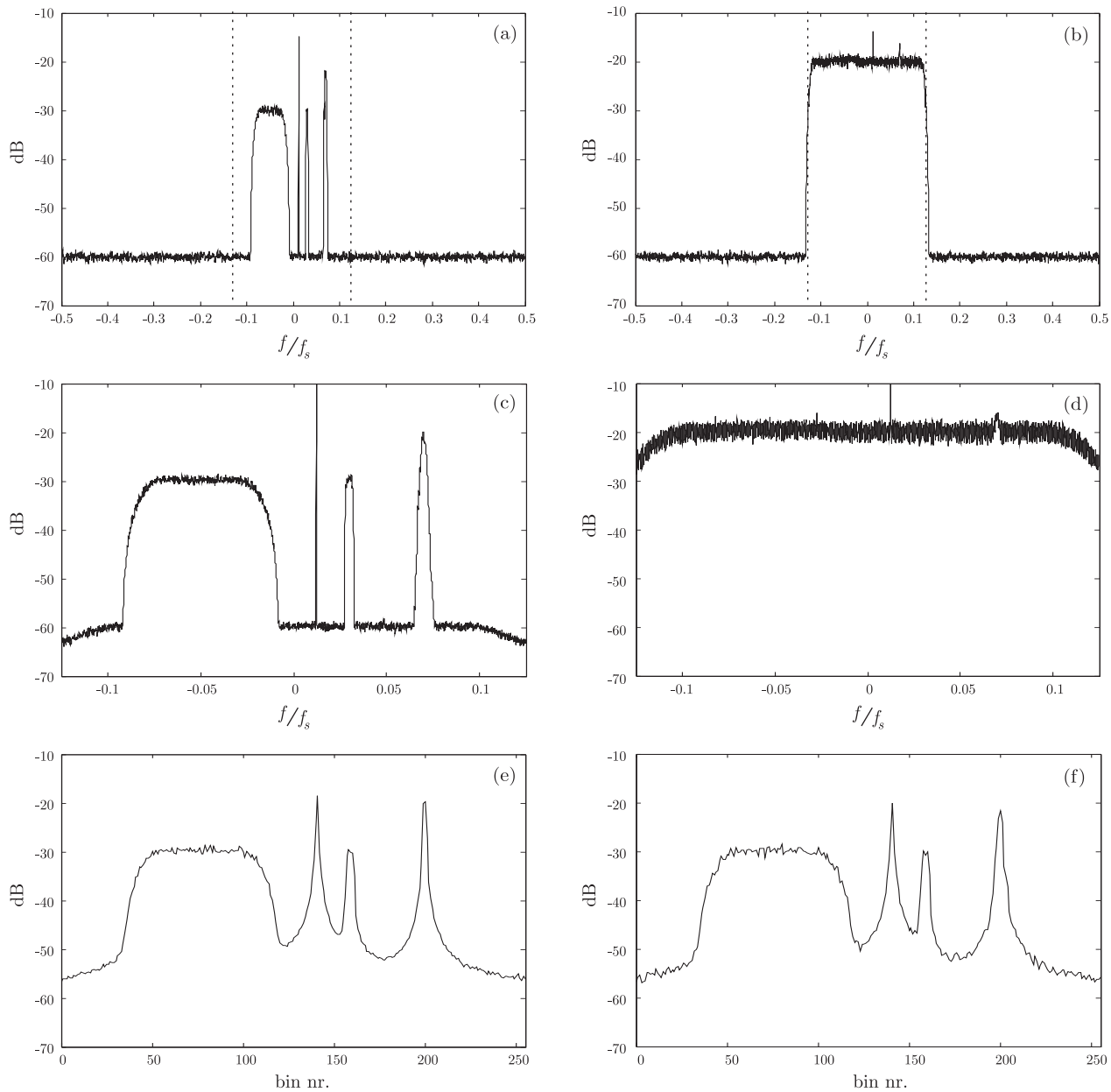

Fig. 4. Simulation results: (a) Welch estimation of the full IF bandwidth with four primary users. (b) is the same as (a) but with an active cognitive radio signal. (c) and (d) are similar to (a) and (b) but after down-sampling to the OFDM bandwidth. (e) is similar to (c) but without a tapering window and only 256 FFT bins. (f) Spectrum estimation of the proposed method, with L = 256 and N = 100.

$$\mathrm{E}\left\{|U[k]|^2\right\} \;=\; \sum_{i=0}^{L-1} \;\mathrm{sinc}(i-k+\frac{f_o}{\Delta f})^2. \qquad (11)$$

The second therm is more difficult, because it involves a square root operation,

$$\mathrm{E}\left\{|U[k]|\right\} \;=\; \mathrm{E}\left\{\sqrt{U[k]\;U[k]^*}\right\}. \qquad (12)$$

If the frequency offset is much smaller than the inter carrier spacing, we can approximate (11) and (12) by only one sinc function, and we get

$$\hat{S}_{\text{self_noise}}[k] \;\approx\; 2\left(\mathrm{sinc}(\frac{f_o}{\Delta f})^2 \;-\; \mathrm{sinc}(\frac{f_o}{\Delta f})\right). \qquad (13)$$

In Fig. 6 we plot this self-noise estimation as function of the frequency offset, and also plot some measured values. We see that the curve falls off with a slope of 20 dB per decade. The vertical scale is relative to the OFDM signal, so a self-noise of 0 dB means that the self-noise has the same magnitude as the OFDM signal. In our example, where we have an SNR of 40 dB, we can read from the plot that the self-noise would be at the same level as the noise floor at a frequency offset

978-1-4244-4148-8/09/$25.00 ©2009
This full text paper was peer reviewed at the direction of IEEE Communications Society subject matter experts for publication in the IEEE "GLOBECOM" 2009 proceedings.

of about 1/178 bin size. This accuracy is easily obtained with a standard frequency offset estimator that correlates between two identical training symbols in the preamble.

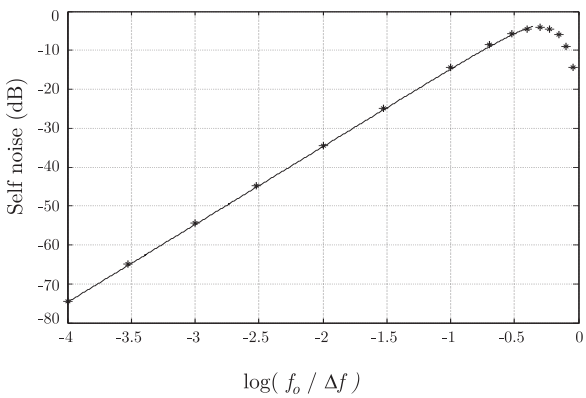

Fig. 6. Self-noise caused by frequency offset. The markers indicate measured values, the line indicate the approximate theoretical value.

VI. Measurements

Besides a frequency offset, a receiver will also have phase-noise, quadrature imbalance and other impairments. To verify that the detection algorithm works with real hardware, we tested it with two USRP [5] transceivers with FLEX-400 RF daughter boards.

The cognitive radio OFDM signal, as described in section IV, was transmitted over a distance of about 30 m in an indoor environment. In order to prevent actual interference to real primary users outside the building, we used a low transmit power. Fig. 7 shows the results. Fig. 7b shows a spectrum measurement when the cognitive radio is silent. At least six narrow band primary users are visible. The exact origin of these signals is unknown, but typical usage of the 450 MHz band is land mobiel radio. Fig. 7c shows the spectrum measured with our method, while the cognitive radio transmitter is active. This measurement was made a few seconds after (b), so some signals are different.

VII. Discussion and conclusion

In this paper we describe a simple but effective in-band sensing system that can function while the systems own signal is active. The advantage of such method in general is that it reduces the chance of missing a primary user that only transmits short signal bursts. The advantage of our method over the system described in [2] is that it has a lower complexity, because no accurate channel estimations are required. The advantage over the method described in [3] is that we perform continuous sensing on all the sub-carrier instead of dedicated sensing carriers. The main disadvantage of our method is that the sub-carrier modulation is restricted to phase shift keying. This gives a lower spectral efficiency than typical QAM16 and QAM64. It should be noted, however, that QAM64 in practice only works under good channel conditions, and typical implementation often switch back to lower order modulations.

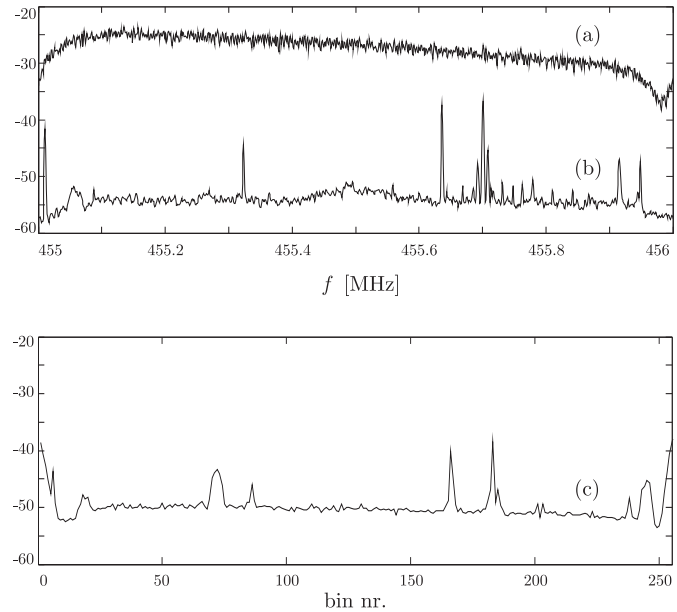

Fig. 7. Measurements with USRP. (a) Welch estimation when OFDM signal is active; The primary users are obscured. (b) Spectrum when OFDM signal is turned off. (c) Spectrum measured with proposed method when the OFDM signal is active.

So, basically we restrict our self to a spectrum efficiency of 2 bit/s/Hz instead of the 4 bit/s/Hz of QAM16 or 6 bit/s/Hz of QAM64. On the other hand, very spectrum efficient schemes may not by too suitable for secondary spectrum usage by cognitive radio anyway, because they need relatively much transmit power, which increases the interference level over a wider area. The differential encoding of the PSK symbols cost approximately 2.125 dB more transmit power than a scheme with QPSK with pilot tones for phase tracking.

References

[1] FCC, "Facilitating opportunities for flexible, efficient, and reliable spectrum use employing cognitive radio technologies," ET Docket No. 03-108, December 2003, notice of Proposed Rulemaking (NPRM).

[2] Baowei Ji and Yinong Ding and David Mazzarese, "Channel Sensing Based on Self-Signal Suppression (SSS)," Tech. Rep., www.ieee802.org/22/Meeting_documents.

[3] D. Chen, J. Li, and J. Ma, "In-band sensing without quiet period in cognitive radio," 31 2008-April 3 2008, pp. 723–728.

[4] J. G. Proakis, *Digital Communications*. McGraw-Hill, 2001.

[5] Z. Yan, Z. Ma, H. Cao, G. Li, and W. Wang, "Spectrum sensing, access and coexistence testbed for cognitive radio using usrp," May 2008.

978-1-4244-4148-8/09/$25.00 ©2009
This full text paper was peer reviewed at the direction of IEEE Communications Society subject matter experts for publication in the IEEE "GLOBECOM" 2009 proceedings.